

A Novel Integrity Concept for GBAS Precision Approaches Induced by Error Propagation with Non-Gaussian Distributions

Thomas Dautermann^(*), Boubeker Belabbas and Patrick Rémi
German Aerospace Center (DLR), Germany

1 Abstract and Introduction

In a differential GPS system such as the ground based augmentation system (GBAS) for precision approaches of aircraft, GPS reference stations with known locations are utilized to determine and remove most of the ranging uncertainties of the GNSS system in use. Corrections are broadcast to the aircraft and all but residual errors are eliminated. These residual pseudorange errors are due to the position difference between the aircraft and the reference station and lead to a position uncertainty of the aircraft. To qualify for category I precision guidance, the system has to guarantee that undetected pseudorange errors do not cause horizontal and vertical position errors larger than the horizontal and vertical alert limits with a probability smaller than 2×10^{-7} per approach. There are four fundamental sources of residual pseudorange error for a single frequency GBAS system: signal multipath, receiver noise N_0 , residual troposphere error due to the differential applied troposphere model and the error induced by ionosphere gradients. In this work we combined different theoretical probability density functions (PDF) for each individual error to a combined pseudorange error distribution. This distribution was propagated through the GBAS Hatch filter and

then mapped into the position domain using a one day constellation change observed at Oberpfaffenhofen, Germany (ICAO Identifier EDMO). Where possible, the propagation process was carried out through analytical convolution. When no analytical solution existed, we either performed a numerical solution of the convolution integrals (if the PDF was available in an analytical form) or used numerical convolution for discrete timeseries. The PDF propagation through the Hatch filter was simulated using a pseudo random generator based on the pseudorange error PDF. Our calculations using the unapproximated PDFs yielded a significant reduction of the position domain error at the 2×10^{-7} integrity risk level when compared to classical methods like Gaussian or Gaussian Mixture overbounding.

Indeed, the results suggest a new integrity concept that could be beneficial in obtaining CAT-III performance. The concept employs alert limits and protection levels in the along-track, cross-track and vertical direction rather than the traditional dual split in horizontal and vertical components only. This new concept does not need inflation factors and promises real-time performance through look-up tables. With assumed realistic minimum detectable errors (MDE) for GBAS monitoring algorithms, the position domain error bounds can be reduced even further and decrease close to the projected CAT-III alert limits. This is especially true since the projected

German Aerospace Center (DLR), Oberpfaffenhofen, 82234 Wessling, Germany
(thomas.dautermann@dlr.de)

ionosphere threat space for Europe does not contain the extreme gradients that have been observed over the continental US.

2 Probability Distributions

In this work we use theoretical probability distributions representing four major errors of GBAS positioning induced by multipath, ionospheric gradients, residual tropospheric delay and receiver noise. The multipath error is induced by the reflection of the signal on obstacles, analyzed in detail by Braasch (1996). As described by Pervan et al. (2000) we assume a uniformly distributed phase shift between reflected and original carrier phase. This leads to the following expression for distribution of the multipath error ϵ (for details see Pervan et al., 2000)

$$p_{mp}(\epsilon) = \frac{1}{b^2} \ln \left[\frac{1 + \sqrt{1 - \left(\frac{\epsilon-a}{b}\right)^2}}{\frac{|\epsilon-a|}{b}} \right] \quad (1)$$

where b is the maximum multipath allowed by the correlator spacing of the GPS receiver and a the variable bias of the distribution. For our theoretical example we choose the receiver to have an ultra-narrow correlator spacing and a maximum multipath of 3 m as depicted by the multipath envelope in Novatel (2002) , Since multipath may, in general, be biased we use a symmetry offset from the ordinate of $a = 0.5$ m in the work presented here.

Secondly, the residual ionospheric error is represented by an ionosphere vertical gradient, whose probability distribution has exponential character as shown by Christie et al. (1999) and more recently confirmed by Mayer et al. (2008). Here, we use the exponential distribution for the ionosphere gradient PDF, extracted from Mayer et al. (2008)

$$p_{ivg}(y) = \frac{\ln(10)}{26} 10^{-\frac{|y|}{13}}; \quad (2)$$

where y is the ionospheric gradient in ppm or mm/km.

Extensive research has been performed on the tropospheric effects on GPS which is summarized by Spilker (1996). Based hereupon, the

Radio Technical Commission for Aeronautics (RTCA) has adopted a model for the residual tropospheric error caused by the location difference between aircraft and GBAS ground station (RTCA DO254A (2004), Section 3.3.2.14). It assumes a Gaussian distribution for the error, with a standard deviation dependent on humidity, altitude difference between aircraft and ground station as well as satellite elevation angle. For our computations, we use an altitude of 762 m (2500ft), the approximate altitude at the initial approach fix during precision approaches and a relative humidity of 100%. Moreover, we use receiver noise specifications of the Novatel OEMV-1 positioning engine. These errors are mainly due to thermal and code noise and follow a zero mean Gaussian with a standard deviation of $\sigma_{N_0} = 0.04$ m (Novatel Datasheets). All four PDFs are depicted in Figure 1 on a logarithmic scale.

3 PDF Propagation and Results

Now, we join the individual error distributions to a combined PDF for the pseudorange ρ . We assume each error component to be an individual random variable, the distribution of the sum of those random variables is given by the convolution of the four individual error PDFs.

$$p_{\rho}(\epsilon_{\rho}) = \int \int p_{ion}(\epsilon_{\rho} - \tau - \lambda) p_{mp}(\tau) p_{tropo+C/N_0}(\lambda) d\tau d\lambda \quad (3)$$

where ϵ_{ρ} is the random variable for the pseudorange error. The ionosphere PDF p_{ion} is computed from the ionosphere gradient PDF p_{ivg} at a worst case distance of 20 nautical miles from the GBAS station. Convolving the tropospheric and N_0 noise PDFs to a joint distribution $p_{tropo+N_0}$ is trivial and accomplished by variance addition. We solve the integral in Eq. (3) numerically with a precision of 1 mm for ϵ_{ρ} . The resulting distribution is shown in Figure 2 in purple for a satellite elevation angle of 5° . In general, this PDF depends on the distance of the aircraft from the GBAS station and

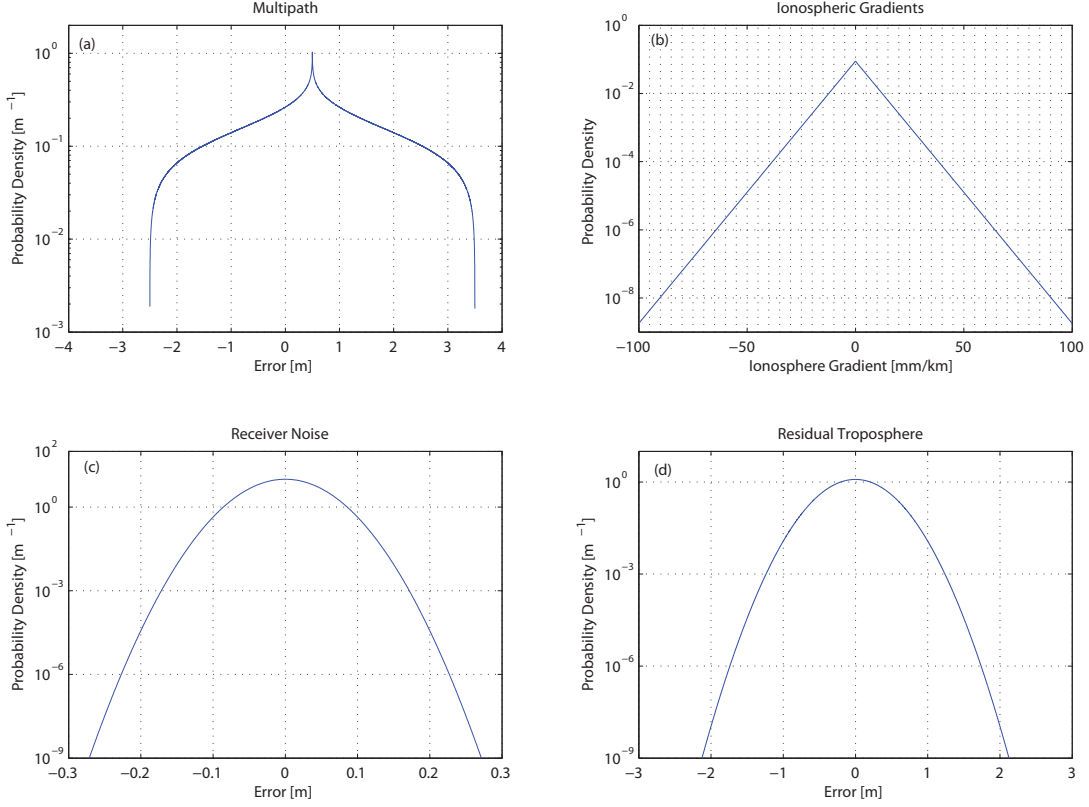


Figure 1: The four error distributions used in this work. (a) shows the multipath distribution described by Eq. (1) with the multipath cutoff at $b=3m$ and a bias of $a = 0.5 m$. (b) the exponential distribution of the ionospheric gradients (c) Gaussian receiver noise PDF with $\sigma = 0.04 m$ (d) Gaussian residual troposphere error distribution for an elevation angle of 5° amounting to $\sigma = 0.252 m$.

satellite elevation angle. The symmetry axis of the PDF is still offset from the origin and located at $0.499 m$. The GBAS ground subsystem employs a 100s carrier-phase smoothing filter (Hatch filter) as, for example, defined in the ED-114 GBAS MOPS (2003), Chapter 3.7.1.2.8.3.5:

$$\hat{\rho}_n = \alpha \rho_n + (1 - \alpha) \left(\hat{\rho}_{n-1} + \frac{\lambda}{2\pi} (\phi_n - \phi_{n-1}) \right) \quad (4)$$

where $\hat{\rho}_n$ is the smoothed pseudorange, ρ_n is the raw pseudorange, $\lambda = 0.19 m$ is the L1 wavelength, ϕ_n is the carrier phase in radians and $\alpha = 0.005$ is the filter weighting constant. Since this filter is recursive, one cannot find an analytical solution for a general error distribution. Note, however, that this is possible for purely Gaussian modes. Thus, we used a

pseudorandom generator with the underlying combined distribution $p_\rho(\epsilon_\rho)$ (computed using Equation 3) to generate 10^9 random samples, which equals about 15.9 years of data recorded at $2 Hz$. From this we can empirically generate a post-smoothing PDF using binning. This distribution is shown in Figure 2 with a green line. We can see that the smoothing filter reduces the width of the pseudorange PDF and thus the probability for larger errors.

Next, we map the error distributions into the position domain using a worst case geometry observed at Oberpfaffenhofen airport (ICAO Identifier EDMO). The mapping is performed using

$$\epsilon_x = \underbrace{(G^T W G)^{-1} G^T W}_S \epsilon_\rho \quad (5)$$

with the geometry matrix G in the east-north-up coordinate system, weighting matrix W , pseudo-inverse S and pseudorange error $\epsilon_{\hat{\rho}}$ to yield the position error ϵ_x . Since the GPS constellation approximately repeats at the same location every 24 hours we performed a geometry screening for that period and selected the constellation with the largest vertical dilution of precision (VDoP). This occurred at 12:45 UT with $n = 7$ satellites in view and an VDoP of 4.32. The pseudoinverse is given in the appendix. The error in each position coordinate $x_i, (i = 1, 2, 3)$ is a weighted sum of random variables

$$\epsilon_{x_i} = \sum_{j=1}^n S_{ij} \epsilon_{\rho,j} = \sum_{j=1}^n \epsilon_{ij} \quad (6)$$

where the S_{ij} are elements of the pseudoinverse. Again, we have assumed the pseudorange errors to be independent. To obtain the PDFs for each component, we first compute the new probability distribution for each new variable $\epsilon_{ij} = S_{ij} \epsilon_{\rho,j}$ following Schmidt (2003)

$$p(\epsilon_{i,j}) = \frac{1}{|S_{ij}|} p\left(\frac{\epsilon_{\rho,j}}{S_{ij}}\right) \quad (7)$$

given the distribution of $\epsilon_{\rho,j}$ from Equation (3). These new distributions are now combined through $n - 1 = 6$ convolutions to a final probability density distribution for position error $\epsilon_{x,i}$.

The error distributions for the east, north and up position components are shown in Figure 3(a) on a semi-logarithmic scale. As expected the Up component PDF is much wider than the one for East or North due to the satellite geometry. North and East component distributions are not equal, but their difference is much smaller compared to the difference between each horizontal and the vertical PDF. Intriguingly, through the process described by Equation (7) and the subsequent convolutions, the initial bias originating from the multipath distribution (Eq. 1) which was still visible in the joint pseudorange PDF (Figure 2) has diminished to a value smaller than our working precision of 1 mm. Since S contains,

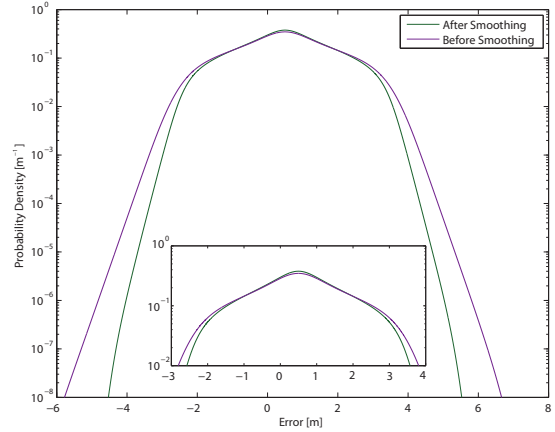


Figure 2: Pseudorange PDFs before and after the carrier smoothing process. The filter narrows the tails of the distribution.

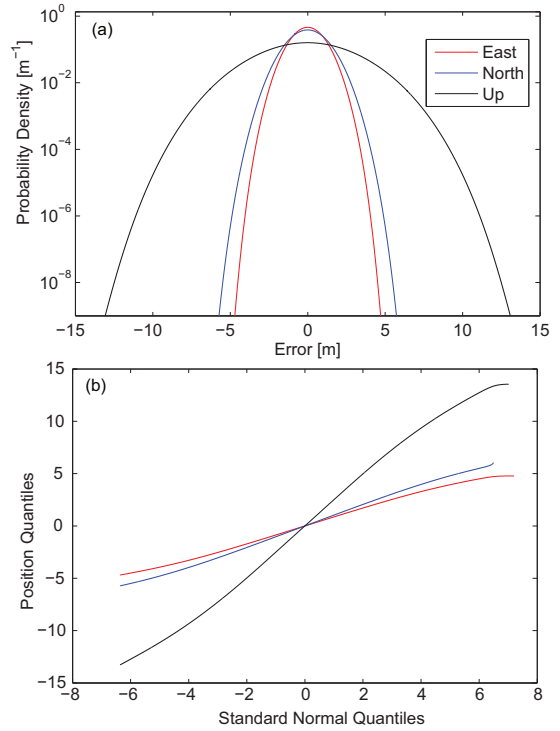


Figure 3: (a) Position Domain Error Distributions on a logarithmic axis (b) Quantile plots of the biased position domain error distributions with standard normal quantiles on the abscissa. Gaussian distributions appear as straight lines.

for a given position component i , a roughly equal number of positive and negative values, Equation (7) causes the distributions $p(\epsilon_{i,j})$ to have the same number of positive and negative biases. In the subsequent convolution processes, the biases cancel and the resulting PDF is centered around the ordinate. Additionally, the distributions shown in Figure 3(a) appear to be Gaussian on the semilogarithmic plot. To confirm this, we inspect quantile-quantile graphs with standard Gaussian quantiles on the x-axis. In this type of plot, any Gaussian PDF will appear as a linear function (Figure 3(b)). Indeed, here the distributions are almost straight, with a very faint curvature. This indicates that even though the position error distributions are very close to being Gaussians, there is a non-normally distributed component present.

4 Outlook

In this work we considered four pseudorange error sources of which two were non-Gaussian and with one of the later also having a bias of 0.5 m. Through the propagation process the non-Gaussian elements and the bias were mitigated and the resulting position error PDFs are nearly normal distributions again. This result confirms the fact predicted by the central limit theorem: Given a sufficiently large set of independently distributed random variables, the PDF of the sum will be Gaussian. This is exactly the case here, with "sufficiently large" being accomplished already with seven independent random pseudorange errors.

Figure 4 shows the error ellipsoid with colored isoprobability contours for the distributions computed above. We can see that already here, at the 20 nm distance and 2500 ft altitude we obtain a maximal vertical error of 12.2 m at the 2×10^{-7} integrity risk level. This is well below CAT-I minimums required at this distance and altitude and nearly enough to suffice the requirements at decision height. Moreover, it is significantly better that the current protection levels given by the standardization documents from RTCA DO-254A (2004) and

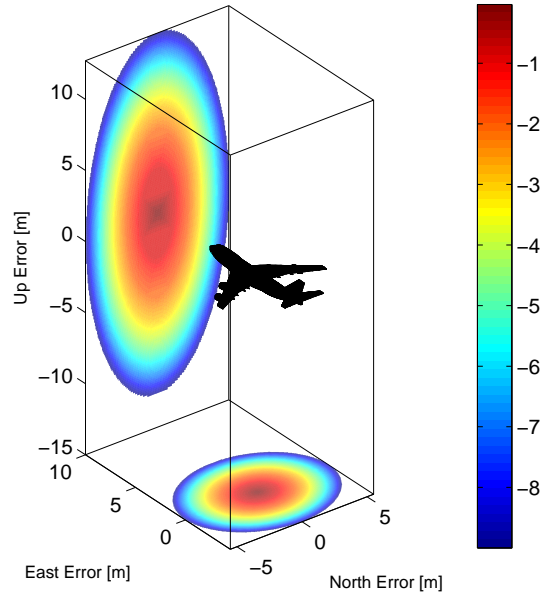


Figure 4: Ellipsoidal iso-probability contours for the worst VDOP Value at EDMO at a distance of 20 nm and altitude of 2500 ft. The colorbar shows the \log_{10} of the probability.

EUROCAE ED-114 (2003). Notwithstanding the fact that the overbounding techniques developed by DeCleene (2000) are sufficient to guarantee CAT-I performance, with the advent of GBAS CAT-III plus automatic landing this integrity concept will no longer provide sufficient performance. In this sense, we suggest an ellipsoidal protection level concept around the along-track, cross-track and vertical axes. This has the advantage of being able to accommodate biased distributions, in the case of insufficient random variables available for addition. Moreover, in the present concept, a cylindrical protection volume is fitted into the protection ellipsoid, which effectively wastes protection space where errors would still be acceptable.

Acknowledgements The authors would like to thank Anja Grosch for her constructive review and Thomas Flament for his support with the geometry screening at EDMO.

5 Appendix

The pseudoinverse used in section 2 contains the following values

$$S = \begin{pmatrix} 0.1546 & 0.2210 & 0.3484 & \dots \\ 0.2690 & -0.3216 & -0.0683 & \dots \\ -0.9214 & 0.3657 & 0.2349 & \dots \\ -0.4914 & 0.3773 & 0.2642 & \dots \\ -0.3598 & 0.1344 & -0.0925 & -0.4061 \\ 0.4422 & 0.3407 & -0.4535 & -0.2085 \\ 0.6366 & 0.3859 & -1.4674 & 0.7657 \\ 0.5477 & 0.3410 & -0.7338 & 0.6950 \end{pmatrix} \quad (8)$$

References

- [1] M. Braasch. *Global Positioning System: Theory and Applications*, chapter Multipath Effects, pages 547–568. AIAA Progress in Aeronautics and Astronautics, 1996.
- [2] Jock R. I. Christie, Ping-Ya Ko, Andrew Hansen, Donghai Dai, Samuel Pullen, Boris S. Pervan, and Bradford W. Parkinson. The Effects of Local Ionospheric Decorrelation on LAAS: Theory and Experimental Results. In *ION NTM*, 1999.
- [3] Bruce DeCleene. Defining Pseudorange Integrity Overbounding. In *ION GPS*, 2000.
- [4] EUROCAE. ED-114: Minimum Operational Performance Specification for Global Navigation Satellite Ground Based Augmentation System Ground Equipment towards Support Category I Operations. Technical report, EUROCAE, 2003.
- [5] C. Mayer, N. Jakowski, C. Borries, T. Pannowitsch, and B. Belabbas. Extreme ionospheric conditions over Europe observed during the last solar cycle. In *Navitec*, number S08-01. European Space Agency, 2008.
- [6] Novatel. *Local Area Augmentation System (LAAS) Ground Facility (LGF4) Reference Receiver*, om-20000070 edition, 12 2002.
- [7] Boris Pervan, Sam Pullen, and Irfan Sayim. Sigma Estimation, Inflation, and Monitoring In the LAAS Ground System. In *ION GPS*, 2000.
- [8] RTCA/SC-159. RTCA/DO-245A: Minimum Aviation System Performance Standards for the Local Area Augmentation System (LAAS). Technical report, RTCA, 2004.
- [9] Volker Schmidt. *Wahrscheinlichkeitrechnung*. Universität Ulm, 2003.
- [10] J. J. Spilker. *Global Positioning System: Theory and Applications*, chapter Ionospheric Effects on GPS, pages 517–546. AIAA Progress in Aeronautics and Astronautics, 1996.